Breakdown of Time–Temperature Superposition in Miscible Polymer Blends and the Coupling Scheme

K. L. Ngai*

Naval Research Laboratory, Washington, D.C. 20375-5000

D. J. Plazek

Material Science and Engineering Department, University of Pittsburgh, Pittsburgh, Pennsylvania 15261

Received November 18, 1989; Revised Manuscript Received March 23, 1990

ABSTRACT: The coupling theoretical scheme has been used to describe the terminal as well as the softening dispersion of a miscible blend of 20 wt % poly(ethylene oxide) in poly(methyl methacrylate). Compared with the pure states, the blend has a drastically reduced number of kinetic couplings of PEO chains but a slightly increased number for PMMA chains. This modification of kinetic coupling provides insight into the breakdown of time–temperature superposition in the blend as observed by Colby. Further use of the other consequences of the coupling theory has yielded results that are in agreement with several other features of the experimental data.

Introduction

Rheological properties of miscible (single phase) polymer blends are of both basic and practical importance. Recently, Colby[1] reported dynamic mechanical property data for a miscible blend of 20 wt % poly(ethylene oxide) in poly(methyl methacrylate) at four temperatures well above the glass transition temperature of the blend. The PEO has a weight-average molecular weight M_w of 235 000 and the PMMA has M_w of 107 000. Both of these samples have $M_w/M_n < 1.2$ and hence are not very polydisperse. The molecular weights for effective entanglement coupling M_c from the dependence of viscosity η on molecular weight M are respectively 28 000 for PMMa and 4400 for PEO. Hence $M_w/M_c \gg 1$ for both pure components so they are entangled. Colby found that the principle of time–temperature superposition failed dramatically for his miscible blend in the terminal region of response, contrary to previous data on single-phase blend systems which indicated that time–temperature superposition was applicable. Colby explained that this breakdown was not found previously because previous experiments were carried out with considerably narrower ranges of frequency and on blends with polydisperse components and were confined to considerably narrower ranges of temperature. Polydispersity of the pure components tends to obscure the failure. Moreover, Colby has studied a number of PEO/PMMA blends of different molecular weights and compositions, and time–temperature superposition failed for all of these blends. Thus the effect observed appears to be real and requires further analysis.

Let us summarize three essential features observed together with the breakdown of time–temperature superposition in the PEO/PMMA blends.

(1) The terminal relaxation of the blend is due to the terminal relaxation of the PMMA molecules, and the maximum in $G''(\omega)$ at somewhat higher frequencies is due to the terminal relaxation of the PEO molecules. The terminal relaxation time of PEO is observed to be shorter than that of PMMA. However, the path length L (in the context of the tube model) and the chain length $L_0 \equiv M/M_0$ of pure PEO are longer than those of pure PMMA, and one would expect in the blend the terminal relaxation time of PEO to be longer than that of PMMA, contrary to experimental data. Henceforth we shall refer to this unexpected feature of the experimental data as *reversal in time scales*.

(2) The temperature dependences of the shift factors a_T(PEO) and a_T(PMMA) for the two components in the blend are quite different, with a_T(PMMA) having a steeper temperature dependence (see Figure 2 of ref 1).

(3) We notice in the blend time–temperature superposition fails not only because the terminal relaxations of the two components have different shift factors but also because the softening dispersion (i.e., the rapidly rising part of the loss modulus curve with $G''/10^5$ (dyn/cm^2) $\geq$ 30 in Figure 1 of ref 1) has another totally different shift factor. This is evident by inspection of Figure 1 of ref 1 in which loss modulus data at four temperatures for the blend when shifted by a_T(PMMA) on the frequency scale superpose well for the terminal relaxation due to relaxation of the PMMA but not for the relaxation of the PEO and the softening dispersion at the highest frequencies. In this plot, the local maximum due to PEO moves to lower frequencies at higher temperatures. On the other hand, the softening dispersion moves in an opposite way to higher frequencies at higher temperatures. By extrapolating the 155 °C loss modulus data to higher frequencies, we have determined in addition the shift factor for the softening dispersion at the highest measured loss modulii. The results are shown in Figure 1 where against temperature we plot the shift factor a_T(S) for the softening dispersion and the shift factors for the two terminal relaxations previously determined by Colby, using a reference temperature of 155 °C. The plot demonstrates that three different temperature dependences are involved, with the temperature dependence of a_T(S) being the strongest. This means that not only the terminal relaxation of each component in this miscible blend has its own effective friction coefficient but also the softening dispersion has a totally different effective friction coefficient.

The first feature of reversal in time scales observed by Colby in rheology has been seen earlier by Composto et al.[2] by measuring tracer-diffusion coefficients D^* of deuterated poly(2,6-dimethyl-1,4-phenylene oxide) and deuterated polystyrene diffusing into blends of undeuterated PS:PXE. D^* for the 35 000 d-PXE component was found to be about a factor of 80 lower than D^* for the

0024-9297/90/2223-4282$02.50/0

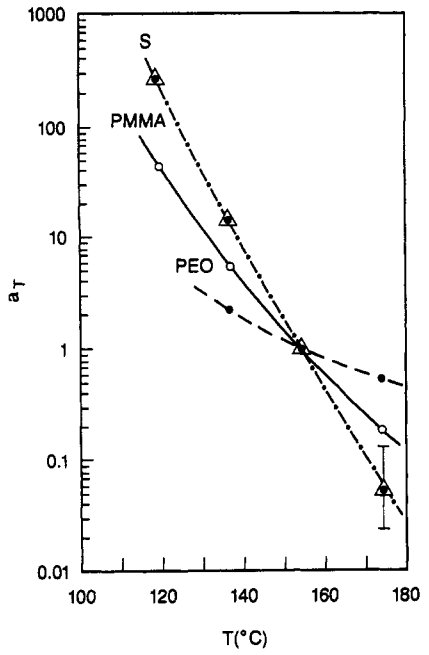

Figure 1. Temperature dependence of shift factors a_T for both components in the blend from Colby:[1] (○) PMMA; (●) PEO. Also included is the temperature dependence of shift factor a_T for the softening dispersion (▲). Lines are drawn to guide the eyes.

255 000 d-PS component in the lower volume fractions of PS.

As pointed out by Colby, current molecular theories of polymer relaxation based on chain reptation[3] in the confining tube made up of other chains assumed that there is only one effective friction coefficient. An exception is the consideration of the mutual diffusion coefficient of two compatible polymers by Brochard-Wyart[4] in which three microscopic friction coefficients are used. Multiple friction factors could result in the reversal in time scales. At this time, the idea has not yet been developed to address the problem of our present interest. In all other tube models[3] the rheological temperature dependences in these models are determined by *one* effective friction coefficient. However, Colby's data of the miscible blend indicate each component has its own individual effective long-range friction coefficient. Moreover, we find that these two individual friction coefficients are both different from the effective friction coefficient of the common softening dispersion. Obviously, current molecular theories[3] cannot explain these three features of the breakdown of time–temperature superposition displayed in Figure 1. This paper is an attempt to see if the coupling theoretical scheme can interpret these experimental facts.

In this work we apply the coupling theoretical scheme[5,6] to the miscible polymer blends studied by Colby to account for the three features observed in the breakdown of time–temperature superposition. The method we use is a general theoretical scheme of treating relaxation problems in complex correlated (i.e., mutually constrained) systems. Rheological and viscoelastic properties of polymers and polymer blends are examples of relaxations in complex correlated systems. The correlations are provided by the entanglement couplings between polymer chains for relaxations in the terminal zone and by crowding coupling for relaxations in the softening zone. The present authors previously in collaboration with others had applied the coupling model to both the terminal relaxation[7-9] and the viscoelasticity of glass-to-rubber transition[10,11] (i.e., the softening dispersion). The coupling model has been described in these publications, and there is no need to reproduce this description in its entirety here. For terminal relaxation the gist is that the relaxation rates of the Rouse modes (in the modified Rouse theory for undiluted polymers; see Chapter 10 of Ferry's text)[13] are slowed down by the mutual constraints between chains due to entanglement couplings. The effect is most important for the terminal Rouse mode, which has relaxation rate W_0 given by the reciprocal of its relaxation time

$$\tau_0 = a^2M^2\zeta_0(T)/6\pi^2M_0^2RT \tag{1}$$

This rate is slowed down to the form

$$W(t) = W_0(\omega_c t)^{-n_\eta} \tag{2}$$

where ω_c^{-1} is the time scale at which entanglement couplings start to slow down the Rouse rate and n_η is the coupling parameter. The subscript η is used to remind us of the terminal shear relaxation. The order of magnitude of ω_c is ca. 10^9–10^{10} s^{-1}, characteristic of cooperative relaxations that involve entanglement interactions.[5,14] For a monodisperse homopolymer melt with no distribution in W_0, the terminal relaxation from the plateau modulus G_N level is

$$G(t) = G_N F(t) \tag{3}$$

where $F(t)$ is the solution of the equation

$$dF/dt = -W_0(\omega_c t)^{-n_\eta}F \tag{4}$$

for the slowed-down Rouse mode. The solution $F(t)$ is the stretched exponential function

$$F(\tau) = \exp[-(t/\tau_\eta^*)^{1-n_\eta}] \tag{5}$$

where the terminal relaxation time τ_η^* is related to the Rouse relaxation time τ_0 by the "second relation":

$$\tau_\eta^* = [(1-n_\eta)\omega_c^{n_\eta}\tau_0]^{1/(1-n_\eta)} \tag{6}$$

From the dependences of τ_0 on molecular weight M and temperature T, the latter mainly through the primitive (i.e., before entanglement coupling is considered) friction factor $\zeta_0(T)$, the second relation (6) provides predictions of the M and T dependence of τ_η^* as

$$\tau^* \propto M^{2/(1-n_\eta)}[\zeta_0(T)]^{1/(1-n_\eta)} \tag{7}$$

The shift factor a_{T_η} for a reference temperature T_0 is essentially given by

$$a_{T_\eta} = [\zeta_0(T)/\zeta_0(T_0)]^{1/(1-n_\eta)} \tag{8}$$

The coupling scheme obtains general form of the rate slowing down, eq 2, from general physical principles, but alone it does not provide a calculation of the coupling parameter n_η for a realistic polymer system. From Monte Carlo simulations of the dynamics of dense packed linear polymer chains one can calculate the end-to-end vector correlation function $\rho(t)$ as an approximation for $F(t)$. Remarkably, it was[15] found that $\rho(t)$ is in fact a stretched exponential function as predicted by eq 5, and the fractional exponent $1-n_\eta$ is in the neighborhood of 0.6. Prior to this new development in the Monte Carlo simulations that can help us to calculate n_η, meaningful progress[7-11] had been made by the coupling scheme even without the help of Monte Carlo simulations. This is possible because the coupling scheme has multiple independent predictions, e.g., eqs 5 and 7, based on the *same* n_η. One can use one of these predictions, say eq 5 on the shape of the terminal relaxation, to determine n_η by comparing with experimental measurements of $G^*(\omega)$, $J(t)$, or $G(t)$ of monodisperse polymer melt.[5,7-10] With

the n_η determined (n_η lies within the narrow range $0.40 \leq n_\eta \leq 0.45$ from previous works) in this manner, other predictions such as the molecular weight and temperature dependences from eq 7 become explicit (e.g., $M^{3.4}$ for $n_\eta = 0.41$) and offer themselves as critical tests of the coupling scheme. Their good agreements with experimental data indicate that this is a viable approach. With the advent of Monte Carlo simulations of Skolnick et al.[16] and Pakula et al.[15] and molecular dynamics simulations of Kremer et al.,[17] various correlation functions can be calculated and the coupling parameters n_η and n_D (for self-diffusion) obtained. These recent advances make possible the computation of the coupling parameter n of the coupling scheme.

Another example of how we determined the coupling parameter n by comparing one prediction with experimental data and use this same value of n in another prediction or predictions to explain additional experimental fact or facts can be found in ref 9, which discusses self-diffusion in entangled polymer melts. For self-diffusion in monodisperse polyethylenes and hydrogenated polybutadienes, the temperature dependence of the diffusion coefficient D provided a way[9] to determine the coupling parameter n_D for self-diffusion, which turns out to be 0.32. Using this *same* value of n_D, we were able to predict the molecular weight dependence of D to be M^{-2}. Monte Carlo simulations by Kolinski[16] et al. and Pakula et al.[15] and even the molecular dynamics simulation of Kremer et al.[17] at the highest molecular weights they respectively studied have found the mean-square displacement of the center-of-mass $g_{cm}(t) = \langle[\vec{R}_{cm}(t) - \vec{R}_{cm}(0)]^2\rangle$ has the $t^{0.7}$ time dependence over distances such that $g_{cm}(t)$ is larger than the square of a bond distance but less than twice the mean-square radius of gyration. It has been worked out that the coupling scheme predicts[18] $g_{cm}(t) \sim t^{1-n_D}$. Hence on identifying the result of $g_{cm}(t)$ from the coupling scheme with that from the computer simulations, we find the coupling parameter n_D has the value 0.30, which is in good agreement with the value 0.32 we deduced earlier[9] from real experimental data.

The shortcoming of the coupling scheme is that it does not provide a calculation of the value of the coupling parameter n. However, this shortcoming is compensated by the multiple and independent predictions it possesses. Using any one of the several predictions to compare with experimental data, one can determine n. After n is determined, the other predictions now having no adjustable parameter become explicit. If any of these other predictions are in disagreement with the experimental data, the coupling scheme can be rejected. On the other hand, if these other predictons are in accord with experimental data,[5,8-11,14] then it may be legitimate to claim that they and hence the coupling scheme explain the experimental measurements. Moreover, we have seen that there are good agreements also between the correlation function including $g_{cm}(t)$ and $\rho(t)$ calculated by Monte Carlo simulations on the one hand and the corresponding predicted forms by the coupling scheme on the other hand. Hence if we augment the coupling scheme by a Monte Carlo calculation of the correlation function of interest, then the combined effort will provide a calculation of the coupling parameter. Then the second relation, eqs 6–8, will yield quantitative predictions because n_η or n_D is now known.

In the present work on the rheology of miscible blends we do not calculate from first principles the coupling parameters of the terminal relaxations of the PEO and PMMA chains. Nevertheless, the conceptual basis of the coupling scheme will enable us to arrive logically at a clear prediction of how the coupling parameters will change when the pure systems are modified by blending two polymers together. As we shall see the predicted change in n for PEO is in the opposite direction from that for PMMA. The immediate consequences of this result are the breakdown of time–temperature superposition in terminal relaxations and the reversal in time scales. These, together with other predictions, will be discussed in the section to follow.

Coupling Model for Miscible Polymer Blends

The principal result of the coupling scheme, eq 2, is the slowing down of the Rouse rate of any chain by mutual dynamical constraints imposed on all chains by entanglement couplings. In a pure monodisperse polymer, the strength of entanglement coupling remains constant provided the molecular weight M is sufficiently higher than M_c, the "critical" molecular weight for entanglement as determined in a log (viscosity) versus log (molecular weight) plot.[13] This is because as the length of the molecule increases, the number of kinetic couplings defined by the ratio M/M_c increases proportionally. We consider the ratio M/M_c instead of M/M_e, where M_e is the average molecular weight between coupling loci, in accord with the recommendation by Ferry:[13] "Pending better understanding of the relation between M_e and M_c, it is probably desirable to use M_c or jP_c in calculations involving viscosities or frequency scales." In a blend with monodisperse components, each component brings into consideration its own number of kinetic couplings Z/Z_c from its pure state. Here Z is the number of atoms in the backbone of a polymer chain[19] of molecular weight M, and Z_c represents the characteristic value of Z corresponding to M_c. Z is twice the degree of polymerization P_{PMMA} for PMMA and thrice P_{PEO} for PEO. The PEO chains[20] in the pure state have $Z = 16\,023$ and $Z_c = 300$, while the PMMA chains[20] in the pure state have $Z = 2140$ and $Z_c = 560$. The number of kinetic coulings per chain in the pure states are

$$(Z/Z_c)_{PMMA} = 3.8 \tag{9}$$

and

$$(Z/Z_c)_{PEO} = 53.4 \tag{10}$$

and there is a large differential between these two numbers. In the 20 wt % PEO/PMMA blend, a PEO chain has in its neighborhood many PMMA chains that have a much smaller Z/Z_c. These PMMA chains cannot provide a PEO chain in the blend as many kinetic entanglement couplings as other PEO chains can in pure PEO. Let ϕ_{PEO} and ϕ_{PMMA} be the volume fractions in the binary blend, and Z_{PEO} and Z_{PMMA} be the chain atom numbers of the two components. Also let $Z_{c,PEO}$ and $Z_{c,PMMA}$ be the "critical" Z's for entanglement of pure PEO and PMMA, respectively. A reasonable estimate of the number of kinetic couplings of a PEO chain and a PMMA chain in the blend is given respectively by the expressions

$$Z_{PEO}/[\phi_{PEO}Z_{c,PEO} + \phi_{PMMA}Z_{c,PMMA}] \tag{11}$$

and

$$Z_{PMMA}/[\phi_{PEO}Z_{c,PEO} + \phi_{PMMA}Z_{c,PMMA}] \tag{12}$$

For Colby's blend with 20.2% by weight PEO, expression 11 evaluates to 31.6 and expression 12 to 4.2. Comparing these values of the number of kinetic couplings in the blend with their corresponding values in the pure polymers given by eqs 9 and 10, we see in the blend there is a large reduction of the number of kinetic couplings of the PEO chains from 53.4 to 31.6 but a slight increase of the number of kinetic couplings of the PMMA chains from 3.8 to 4.2.

At fixed chain length, the total strength of kinetic entanglement coupling and the coupling parameter n for a chain are increasing functions of the number of kinetic couplings it has. It follows from this reason and the analysis given above that the terminal coupling parameter n_{PEO} for PEO chains in the blend will be reduced significantly from the value of about 0.41 (see previous section and references)[5,7-10] in pure monodisperse linear polymers including PEO. On the other hand, the coupling parameter n_{PMMA} for PMMA chains in the blend will be increased slightly from 0.41. Thus we arrive at the conclusion that in Colby's 20% PEO/PMMA blend

$$n_{PEO} < 0.41 < n_{PMMA} \tag{13}$$

We emphasize that the inequalities given by (13) are derived from the conceptual basis of the coupling scheme and are not ad hoc assumptions.

Next we show the appearance of two different coupling parameters, one for PEO and another PMMA chains, gives rise to two different shift factors a_T(PEO) and a_T(PMMA) for relaxations of PEO and PMMA, respectively, in the blend. This result follows from eq 7 and 8. The Rouse friction coefficient $\zeta_0(T)$ is the *same* for PEO and PMMA chains because the blend is miscible and exhibits one T_g. The two shift factors given by the expressions

$$a_T(\text{PEO}) = [\zeta_0(T)/\zeta_0(T_0)]^{1/(1-n_{PEO})} \tag{14}$$

and

$$a_T(\text{PMMA}) = [\zeta_0(T)/\zeta_0(T_0)]^{1/(1-n_{PMMA})} \tag{15}$$

are therefore different because from inequality 13 n_{PEO} and n_{PMMA} are different in the blend. The breakdown of time–temperature superposition in the blend is thus expected as a consequence of (13), a result derivable in the coupling scheme. Furthermore, inequality 13 enables us to predict a_T(PMMA) is a more rapid varying function of temperature than a_T(PEO) because the exponent $1/(1 - n_{PMMA})$ in eq 15 is larger than the exponent $1/(1 - n_{PEO})$ in eq 14. This prediction is in agreement with what is observed in the experimental data as shown in Figure 1. Moreover, in this figure the shift factor of the softening dispersion a_T(S) has the most rapid temperature variation of all. This will be explained next.

The variation of the shift factor a_T(S) with temperature is determined by the temperature dependence of the relaxation time τ_α^* of the segmental α relaxation time. The segmental relaxation in undiluted polymers involves a different kind of intermolecular coupling to be distinguished from entanglement coupling for terminal relaxation. The coupling scheme being a general physical principle applies also to the segmental relaxation.[5,10,11,14,19] Just as in the case of terminal relaxation the scheme offers a number of predictions. The time dependence of the segmental relaxation is predicted to be another stretched exponential

$$\phi(t) = \exp[-(t/\tau_\alpha^*)]^{1-n_\alpha} \tag{16}$$

which is better known as the Kohlrausch–Williams–Watts (KWW) function for the segmental relaxation. Here, n_α is the coupling parameter for segmental motion due to crowding coupling, the counterpart of n_η for terminal relaxation due to entanglement coupling. There is a corresponding "second relation" analogous to eq 6 relating the experimentally observed relaxation time τ_α^* to the relaxation time $\tau_{0\alpha}$ of segmental motion of a chain before rate slowing down by intermolecular coupling is taken into account. The second relation for segmental relaxation is

$$\tau_\alpha^* = [(1 - n_\alpha)\omega_c^{n_\alpha}\tau_{0\alpha}]^{1/(1-n_\alpha)} \tag{17}$$

which also generates multiple predictions and gives rise to several applications.[5,10,11,14,21,22] The crossover frequency ω_c for segmental relaxation may be different from that for terminal relaxation.

Applying eqs 17 and 6 to the blend, we shall explain why the temperature dependence of τ_α^* described by the shift factor a_T(S) of the softening dispersion is different from that of the terminal relaxation time τ_η^* and is shift factor $a_{T\eta}$. Associated with the softening dispersion contributed by the motions of polymer molecular segments in the blend, there is a crowding coupling parameter n_α. In the past, we have determined n_α by fitting eq 16 to dielectric, photon correlation spectroscopic, and shear creep compliance data and found that it is significantly larger than n_η. For example, $n_\alpha = 0.63$ for polystyrene (PS),[10] 0.64 for atatic polypropylene (PP),[21] 0.64 for poly(cyclohexyl methacrylate),[18] and 0.57 for poly(vinyl acetate) (PVAc).[10] Thus from previous works in the pure state,[5,10,19] we found that $n_\alpha > n_\eta$. Typically, $n_\alpha \simeq 0.6$ and as we have discussed $n_\eta = 0.41$. This result applies also to the blend, and combining with (13), we arrive at the inequalities

$$n_\alpha > n_{PMMA} > n_{PEO} \tag{18}$$

The friction coefficient of $\tau_{0\alpha}$ in eq 17 is the same[10,11] as that (i.e., ζ_0) of the Rouse relaxation time τ_0 in eq 6. It follows from eq 17

$$\tau_\alpha^* \propto [\zeta_0(T)]^{1/(1-n_\alpha)} \tag{19}$$

and the shift factor for the softening dispersion has the temperature dependence of

$$a_T(\text{S}) = [\zeta_0(T)/\zeta_0(T_0)]^{1/(1-n_\alpha)} \tag{20}$$

Comparing this with eqs 14 and 15 for $a_{T\eta}$, it follows from inequality 18 that the three shift factors a_T(S), a_T(PEO), and a_T(PMMA) are all different. Among them, a_T(S) has the most rapid temperature variation because the exponent $1/(1 - n_\alpha)$ is largest. This difference between a_T(S) and $a_{T\eta}$ has been observed for several pure polymers including PS, PVAc, PP, and others.[5,10,21-25] Previously, we[5,10,21,22] used eqs 8 and 19, together with the known coupling parameters n_α and n_η for a pure polymer, to account quantitatively for the difference of the two shift factors in pure polymers.

The same analysis can be applied to the miscible blend PEO/PMMA provided we know n_α for the segmental α relaxation. At present, the shear viscoelastic data of Colby in the softening region are not extensive enough in frequency for a determination of n_α from his experimental data. To make progress, we shall assume in this work a value of 0.66 for n_α in the blend. This value is close to the value n_α for pure PMMA. We use the same reference temperature T_0 of 155 °C for a_T(PEO), a_T(PMMA), and a_T(S) given by eqs 14, 15, and 20, respectively. The data for a_T(S) as shown in Figure 1 and the value $n_\alpha = 0.66$ enable us to determine from it the primitive shift factor $\zeta_0(T)/\zeta_0(T_0)$ for three temperatures, 120, 137, and 155 °C, by inverting eq 20. With $\zeta_0(T)/\zeta_0(T)$ determined, Colby's data of a_T(PEO) and a_T(PMMA) are substituted into the left-hand sides of eqs 14 and 15, respectively, and we solve for n_{PEO} and n_{PMMA} in his blend. The results found are

$$n_{PEO} = 0.16 \tag{21}$$

and

$$n_{PMMA} = 0.46 \tag{22}$$

We emphasize that these values for the coupling parameters are not arbitrary but are calculated by using the predicted relations (14) and (15) provided by the coupling scheme from the measured temperature dependences of the three shift factors.

Obviously, these values of the coupling parameters satisfy inequality 13. We recall that (13) was obtained earlier from the conceptional basis of the coupling scheme by arguments based on large reduction and slight enhancement of the number of kinetic couplings of PEO and PMMA chains respectively in the blend. Also inequalities 18 are satisfied as well because n_α is ca. 0.66. Indeed we find a large reduction of the coupling parameter of PEO chains and a moderate increase of the coupling parameter of PMMA chains in the blend from the value of 0.41 for pure monodisperse entangled polymers. These trends are the consequences of the large reduction from 53.4 to 31.6 of the number of kinetic couplings of PEO chains and a corresponding small increase from 3.8 to 4.2 for PMMA chains when going from the pure polymers to the 20% PEO/PMMA blend.

With the values of the coupling parameters n_{PEO} and n_{PMMA} in the blend determined by the temperature dependences of the shift factors, we are now ready to derive the reversal in time scales of τ_η*(PEO) compared with τ_η*(PMMA) and also to predict the terminal relaxation time τ_η*(PEO) of the PEO chains by knowing the terminal relaxation time τ_η*(PMMA) of the PMMA chains. The reversal in time scale is the first in the list of anomalies outlined in the Introduction. The second relations for PEO and PMMA are given by

$$\tau_\eta^*(\mathrm{PEO}) = [(1 - n_{PEO})(\omega_c)^{n_{PEO}}\tau_0(\mathrm{PEO})]^{1/(1-n_{PEO})} \quad (23)$$

and

$$\tau_\eta^*(\mathrm{PMMA}) = [(1 - n_{PMMA})(\omega_c)^{n_{PMMA}}\tau_0(\mathrm{PMMA})]^{1/(1-n_{PMMA})} \quad (24)$$

which are specializations of eq 6 to the binary blend. At 155 °C, τ_η*(PMMA) is ca. 10 s estimated from the loss modulus data of Colby. From previous works,[5,14] an order of magnitude estimate of ω_c is $10^{9.5}$. Substituting these estimates of τ_η*(PMMA), ω_c, and n_{PMMA} from eq 22 into eq 24 and solving for τ_0(PMMA), we find τ_0(PMMA) = 1.5×10^{-4} s. The expression for τ_0 has been given by eq 1, where $\zeta_0(T)$ is the same for both PEO and PMMA in the blend. Taking the ratio, we find

$$\tau_0(\mathrm{PEO})/\tau_0(\mathrm{PMMA}) = \left(\frac{aM}{M_0}\right)^2_{\mathrm{PEO}} \Big/ \left(\frac{aM}{M_0}\right)^2_{\mathrm{PMMA}} \quad (25)$$

The parameters on the right-hand side of this equation are known for each individual component of the blend. Thus, knowing τ_0(PMMA), we can calculate τ_0(PEO) and find the value of 4.8×10^{-3} s. Note that

$$\tau_0(\mathrm{PEO}) \gg \tau_0(\mathrm{PMMA}) \quad (26)$$

is satisfied by the Rouse relaxation times. One may have expected this inequality to be satisfied because PEO has a higher molecular weight and also greater number of entanglements per chain than PMMA. But Colby found that experimentally

$$\tau_\eta^*(\mathrm{PEO}) \ll \tau_\eta^*(\mathrm{PMMA}). \quad (27)$$

This reversal can be shown to follow naturally from the second relation. Indeed, with all quantities that appear on the right-hand side of eq 23 known, τ_η*(PEO) can be evaluated immediately. The value calculated for τ_η*(PEO) at T = 155 °C is ca. 0.10 s, which corresponds to a frequency of 10 rad/s. This predicted location of PEO relaxation in the blend is in good agreement with 6 rad/s at which the local maximum in $G''(\omega)$ was observed at 155 °C by Colby. On the other hand, τ_η*(PMMA) at T = 155 °C is ca. 10 s, which is much longer than τ*(PEO). Thus the reversal in time scales as given by the two inequalities (26) and (27) follows.

Conclusion

By comparing the numbers of kinetic couplings of the polymer chains in the pure states and in the blend, we find the number is drastically reduced and slightly increased respectively for PEO and PMMA chains when going from the pure state to the blend. Within the conceptual foundation of the coupling scheme, reduction of the number of kinetic couplings of the same chain will lead to a decrease in the dynamic constraints and hence the coupling parameter n. Thus on physical grounds we expect a large decrease in the coupling parameter n_{PEO} for PEO chains and a slight increase in n_{PMMA} for PMMA chains in the blend from the value of ca. 0.41 for both pure and approximately monodisperse components. Considering also the segmental α relaxation and its coupling parameter n_α in the context of the coupling scheme, we have established the inequalities $n_\alpha > n_{PMMA} > 0.41 > n_{PEO}$. The latter leads to three different shift factors a_T(S), a_T(PEO), and a_T(PMMA) for the softening dispersion, the PEO, and the PMMA terminal relaxations, respectively, and hence the breakdown of time–temperature superposition as Colby observed. As happened before in previous applications[5,7-11,18,19] of the coupling scheme to problems in polymers and other correlated systems, even though we do not provide a calculation for the coupling parameters n_{PEO} and n_{PMMA} in the 20% PEO/PMMA blend, they can be deduced by applying one prediction of the coupling model to one aspect of the experimental data. Here we use the temperature dependences of a_T(S), a_T(PEO), and a_T(PMMA). The coupling parameter n_α for the segmental relaxation can be determined by fitting part of the relaxation or compliance data of the softening dispersion[5,10,11,18,19] with the KWW function, eq 16. The determined values of n_{PEO} and n_{PMMA} confirm that $n_{PEO} < 0.41 < n_{PMMA}$. Using these values of n_{PEO} and n_{PMMA} determined by the temperature dependences of the shift factors, we can account for yet another aspect of the data, i.e., the location of the PEO relaxation relative to that of the PMMA relaxation and why PEO relaxation occurs at higher frequencies than that of PMMA. The latter is not expected a priori because the PEO chains have a higher molecular weight and a greater number of entanglements per chain than PMMA. As shown, the predicted location of the local maximum in $G''(\omega)$ due to PEO relaxation is in good agreement with experimental data. In a similar way, the coupling model can make further predictions such as the molecular weight dependences of the terminal relaxations of PMMA and of PEO in the blend. Keeping the volume fraction of PEO constant at 20%, the PEO molecular weight dependence of the PEO terminal relaxation is predicted to have the dependence of $M^{2/(1-n_{PEO})} \sim M^{2.4}$, which will be weaker than the $M^{3.4}$ for PEO relaxation in the pure state, while PMMA terminal relaxation will have the $M^{2/(1-n_{PMMA})} \sim M^{3.7}$ dependence. Also we can predict the trend in the change of behaviors of blends with higher or lower PEO weight percentage at constant PEO and PMMA molecular weights. Blends with higher PEO volume fraction will have the separation between τ_η*(PEO) and τ_η*(PMMA) reduced. Ex-

perimental data of these kinds are not available at this time. Experiments may be difficult to carry out in PEO/PMMA blends due to the tendency of PEO to crystallize and may have to be done in other blends. When these measurements become available in the future, we expect the predictions of the coupling scheme that can be made at this time will be able to account for them.

Acknowledgment. We thank Ralph H. Colby for making his experimental data available to us. This work is supported in part by ONR Contract N0001489WX24087 (K.L.N.) and by NSF Grant MSM8517120 (D.J.P.).

References and Notes

(1) Colby, R. H. *Polymer* **1989**, *30*, 1275.
(2) Composto, R. J.; Mayer, J. W.; Kramer, E. J.; White, D. M. *Phys. Rev. Lett.* **1986**, *57*, 1312.
(3) Doi, M.; Edwards, S. F. *The Theory of Polymer Dynamics*; Clarendon Press: Oxford, 1986.
(4) Brochard-Wyart, F. *C. R. Seances Acad. Sci.* **1987**, *305*, 657.
(5) For a review, see: Ngai, K. L.; Rendell, R. W.; Rajagopal, A. K.; Teitler, S. *Ann. N.Y. Acad. Sci.* **1986**, *84*, 150, 321.
(6) Ngai, K. L.; Rajagopal, A. K.; Teitler, S. *J. Chem. Phys.* **1988**, *88*, 5086.
(7) Ngai, K. L.; Rendell, R. W. *Polym. Prepr. (Am. Chem. Soc., Div. Polym. Chem.)* **1982**, *23*, 46.
(8) Ngai, K. L.; Plazek, D. J. *J. Polym. Sci., Polym. Phys. Ed.* **1985**, *28*, 2159.
(9) McKenna, G. B.; Ngai, K. L.; Plazek, D. J. *Polymer* **1985**, *26*, 1651.
(10) Ngai, K. L.; Plazek, D. J. *J. Polym. Sci., Polym. Phys. Ed.* **1986**, *24*, 619.
(11) Ngai, K. L.; Plazek, D. J.; Deo, S. S. *Macromolecules* **1987**, *20*, 3046.
(12) Rouse, P. E. *J. Chem. Phys.* **1953**, *21*, 1272.
(13) Ferry, J. D. *Viscoelastic Properties of Polymers*; Wiley: New York, 1980.
(14) Ngai, K. L.; Fytas, G. *J. Polym. Sci., Part B* **1986**, *24*, 1683.
(15) Pakula, T.; Geyler, S. *Macromolecules* **1987**, *20*, 2909 and to be published.
(16) Kolinski, A.; Skolnick, J.; Yaris, R. *J. Chem. Phys.* **1987**, *86*, 1567, 7164.
(17) Kremer, K.; Grest, G. *J. Chem. Phys.*, to be published.
(18) Ngai, K. L.; Liu, F. S. *Phys. Rev.* **1981**, *B24*, 1049. Ngai, K. L.; Skolnick, J., to be published.
(19) Berry, G. C.; Fox, T. G. *Adv. Polym. Sci.* **1968**, *5*, 261.
(20) The values of Z and Z_c for PEO are calculated by the formulas $3M/M_0$ and $3M_c/M_0$, respectively, with M = 235 000, M_c = 4400, and M_0 = 44. The values of Z and Z_c for PMMA are calculated by the formulas $2M/M_0$ and $2M_c/M_0$ with M = 107 000, M_c = 28 000, and M_0 = 100.
(21) Floudas, G.; Fytas, G.; Ngai, K. L. *Macromolecules*, in press.
(22) Fytas, G.; Ngai, K. L. *Macromolecules* **1988**, *21*, 804.
(23) Gray, R. W.; Harrison, G.; Lamb, J. *Proc. R. Soc. London* **1977**, *356*, 77.
(24) Cavaile, J. Y.; Perez, J.; Jourdan, C.; Johari, G. P. *J. Polym. Sci., Polym. Phys. Ed.* **1987**, *25*, 1847.
(25) Alberdi, J. M.; Alegria, A.; Macho, E.; Colmenero, J. J. *Polym. Bull.* **1987**, *18*, 39.